Am J Physiol Heart Circ Physiol 297: H375–H386, 2009.
First published May 8, 2009; doi:10.1152/ajpheart.00498.2007.

Effect of early versus late AT_1 receptor blockade with losartan on postmyocardial infarction ventricular remodeling in rabbits

Germán E. González,[1] Ignacio M. Seropian,[1] Maria Laura Krieger,[1] Jimena Palleiro,[1] Maria A. Lopez Verrilli,[2] Mariela M. Gironacci,[2] Susana Cavallero,[3] Luciana Wilensky,[1] Victor H. Tomasi,[1] Ricardo J. Gelpi,[1,*] and Celina Morales[1,*]

[1]*Institute of Cardiovascular Physiopathology and Department of Pathology, School of Medicine, and* [2]*Institute of Biological Chemistry and Physic-chemistry and* [3]*Department of Physiopathology, School of Pharmacy and Biochemistry, University of Buenos Aires, Buenos Aires, Argentina*

Submitted 25 April 2007; accepted in final form 29 April 2009

González GE, Seropian IM, Krieger ML, Palleiro J, Lopez Verrilli MA, Gironacci MM, Cavallero S, Wilensky L, Tomasi VH, Gelpi RJ, Morales C. Effect of early versus late AT_1 receptor blockade with losartan on postmyocardial infarction ventricular remodeling in rabbits. *Am J Physiol Heart Circ Physiol* 297: H375–H386, 2009. First published May 8, 2009; doi:10.1152/ajpheart.00498.2007.—To characterize the temporal activation of the renin-angiotensin system after myocardial infarction (MI) in rabbits, we examined cardiac ANG II type 1 receptor (AT_1R) expression and ANG II levels from 3 h to 35 days. The effects of losartan (12.5 $mg \cdot kg^{-1} \cdot day^{-1}$) on functional and histomorphometric parameters when treatment was initiated early (3 h) and late (*day 15*) post-MI and maintained for different periods of time [short term (4 days), midterm (20 days), and long term (35 days)] were also studied. AT_1R expression increased in the MI zone at 15 and 35 days ($P < 0.05$). ANG II levels increased ($P < 0.05$) in the non-MI zone at 24 h and in the MI zone as well as in plasma at 4 days and then progressively decreased until 35 days. The survival rate was significantly lower in untreated MI and early long-term-treated animals. Diastolic pressure-volume curves in MI at 35 and 56 days shifted to the right ($P < 0.05$). This shift was even more pronounced in long-term-treated groups ($P < 0.05$). Contractility decreased ($P < 0.05$ vs. sham) in the untreated and long-term-treated groups and was attenuated in the midterm-treated group. The early administration of losartan reduced RAM 11-positive macrophages from 4.15 ± 0.05 to 3.05 ± 0.02 cells/high-power field (HPF; $P < 0.05$) and CD45 RO-positive lymphocytes from 2.23 ± 0.05 to 1.48 ± 0.01 cells/HPF ($P < 0.05$) in the MI zone at 4 days. Long-term treatment reduced the scar collagen (MI: 70.50 ± 2.35% and MI + losartan: 57.50 ± 2.48, $P < 0.05$), determined the persistency of RAM 11-positive macrophages (3.02 ± 0.13 cells/HPF) and CD45 RO-positive lymphocytes (2.77 ± 0.58 cells/HPF, $P < 0.05$ vs. MI), and reduced the scar thinning ratio at 35 days ($P < 0.05$). Consequently, the temporal expressions of cardiac AT_1R and ANG II post-MI in rabbits are different from those described in other species. Long-term treatment unfavorably modified post-MI remodeling, whereas midterm treatment attenuated this harmful effect. The delay in wound healing (early reduction and late persistency of inflammatory infiltrate) and adverse remodeling observed in long-term-treated animals might explain the unfavorable effect observed in rabbits.

angiotensin II type 1 receptor blockers

MYOCARDIAL INFARCTION (MI) leads to global structural alterations that involve infarcted as well as noninfarcted areas in a process collectively known as ventricular remodeling (26). The initial phase of remodeling, which starts in the acute phase of the MI, is associated with geometric changes and dilation of the MI zone, as a consequence of injured wall thinning (14, 26). Shortly afterward, this dilation may progress to the whole ventricle, and it is associated with myocyte hypertrophy and fibrosis in the remote zones. These structural changes begin during the initial phase of the healing process of the infarction, contribute to ventricular dysfunction, cause a progression to heart failure, and increase mortality.

The systemic and cardiac renin-angiotensin systems (RAS) are activated post-MI and actively participate in ventricular remodeling, favoring the healing process of the infarcted area as well as myocyte hypertrophy, fibrosis, and most of the events associated with the remodeling of non-MI zones (22, 38). Due to the fact that ANG II, acting mainly through the ANG II type 1 receptor (AT_1R), is the main active peptide of the RAS (20), many researchers have tried to modify the evolution of post-MI remodeling using AT_1R blockers. In this regard, it has been shown that AT_1R blockers effectively reduce hypertrophy and fibrosis in remote zones and might also decrease chronic cardiac dilation (10, 38). Some reports (12, 16) have shown that an early administration of AT_1R blockers after MI also caused a reduction in fibrosis and in the width of the scar. Nevertheless, the timing for the initiation of AT_1R blockade has not been widely studied. Xia et al. (41) demonstrated in rats that therapy with fonsartan, initiated within the first 24 h or after 7 days post-MI, did not modify the morphological aspects associated with chronic remodeling. However, these authors did not study the implications of those drugs on the histological changes of the infarcted zone. Pourdjabbar et al. (30) confirmed that pre- and peri-MI treatment with losartan (Los) exerted no beneficial effects on survival and arrhythmias in the acute period post-MI, and high doses may even be detrimental due to excessive hypotension. In addition, we (12) have previously showed that the administration of Los to rabbits from the beginning of MI increased ventricular dilation. Taking into account the importance of finding the adequate therapeutic window for the beginning of therapy with AT_1R blockers, our aim was to compare the effects of two Los therapy initiation times on functional and histological aspects of chronic remodeling in an experimental model of MI in rabbits. Additionally, our study aimed to determine if the duration of the AT_1R blockade could also influence the progression of remodeling.

METHODS

Experimental model of MI. New Zealand White rabbits (body weight: 2.0–2.3 kg) were anesthetized with a ketamine (75 mg/kg)

* R. J. Gelpi and C. Morales contributed equally to this work.

Address for reprint requests and other correspondence: R. J. Gelpi, Institute of Cardiovascular Physiopathology, Dept. of Pathology, School of Medicine, Univ. of Buenos Aires, J. E. Uriburu 950, Piso 2, Buenos Aires C1114AAD, Argentina (e-mail: rgelpi@fmed.uba.ar).

and xylazine (0.75 mg/kg) solution. Animals were intubated and then mechanically ventilated using a Harvard ventilator (tidal volume: 25 ml) at a respiratory frequency of 34–38 cycles/min. Subsequently, a lateral left thoracotomy followed by a pericardectomy was performed, and ligature of a lateral branch of the left coronary artery using a 6.0 silk thread was performed as previously described (25). Finally, the chest was closed in layers, and animals were allowed to recover from anesthesia in a quiet environment.

Sham-operated animals underwent the same procedure without ligation of the coronary artery. After animals had recovered from anesthesia, they were housed in individual cages until the end of the protocol. All experiments were approved by the Animal Care and Research Committee of the University of Buenos Aires, and this investigation conforms to the guidelines from the American Physiological Society "Guiding Principles in the Care and Use of Laboratory Animals."

Protocols and experimental groups. Ten experimental groups were studied (Fig. 1). Each group was randomized for experiments of ventricular function and histomorphometric analysis according to the following protocols: untreated MI of 35 days of evolution (MI_{35}), MI evolution of 35 days with Los treatment from the beginning of the protocol until *day 35* (MI_{35} + $Los_{[0]}$), MI evolution of 35 days with Los treatment from *day 15* post-MI (MI_{35} + $Los_{[15]}$), untreated MI with 56 days of evolution (MI_{56}), and MI evolution of 56 days with Los treatment from *day 15* post-MI (MI_{56} + $Los_{[15]}$). Furthermore, to investigate the effects of Los therapy initiation times just on survival rate, another group of animals was treated with Los from the beginning of MI until *day 4* and then treatment was discontinued until *day 35* postsurgery, when animals were killed (MI_{35} + $Los_{[0-4]}$). Sham-operated animals of 35 and 56 days of MI evolution were also studied; since the results of these groups were similar, they were pooled into one single sham group. Finally, two groups of animals [untreated MI of 4 days of evolution (MI_4) and Los treatment from the beginning of MI until *day 4* and then discontinued treatment on *day 4* (MI_4 + $Los_{[0-4]}$)] were studied. These animals were killed at 4 days postsurgery to assess the effects of Los on early cellular inflammatory infiltrate in the infarct zone (Fig. 1).

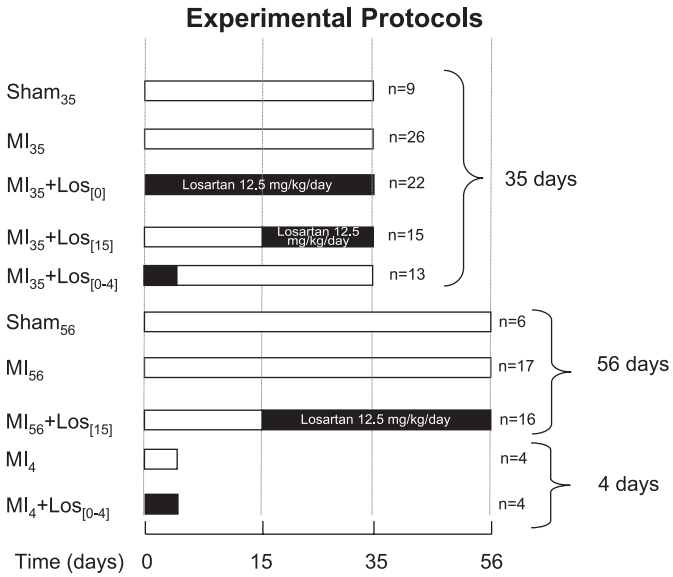

Fig. 1. Experimental protocols. MI, myocardial infarction; Los, losartan. Animals were divided into the following groups: sham treatment of 35 days ($Sham_{35}$) or 56 days ($Sham_{56}$), untreated MI of 35 days of evolution (MI_{35}), MI evolution of 35 days with Los treatment from the beginning of the protocol until *day 35* (MI_{35} + $Los_{[0]}$), MI evolution of 35 days with Los treatment from *day 15* post-MI (MI_{35} + $Los_{[15]}$), Los treatment from the beginning of MI until *day 4* and then discontinued treatment on *day 35* (MI_{35} + $Los_{[0-4]}$), untreated MI with 56 days of evolution (MI_{56}), MI evolution of 56 days with Los treatment from *day 15* post-MI (MI_{56} + $Los_{[15]}$), untreated MI of 4 days of evolution (MI_4), and Los treatment from the beginning of MI until *day 4* and then discontinued treatment on *day 4* (MI_4 + $Los_{[0-4]}$). Results from the $Sham_{35}$ and $Sham_{56}$ groups were pooled (sham group).

To choose the times for beginning the therapy with Los, we used histological criteria based on the temporal histopathological characteristics of MI in rabbits previously described by us (25). Thus, we decided to start therapy at the beginning of the necrotic period, when acute inflammatory infiltrate is not still evident, and on *day 15* post-MI, when the granulation tissue has stabilized and collagen begins to form the scar (25). Hence, we compared the effects of early long-term therapy (MI_{35} + $Los_{[0]}$) with late midterm therapy (MI_{35} + $Los_{[15]}$) as well as with late long-term therapy (MI_{56} + $Los_{[15]}$) on histological, morphological, and functional parameters of post-MI ventricular remodeling. In addition, we also compared the effect of short-term therapy (MI_4 + $Los_{[0-4]}$) on inflammatory infiltrate in the infarct zone and mortality (MI_{35} + $Los_{[0-4]}$). In rabbits, the necrotic stage is mainly characterized by the presence of coagulation necrosis during the first week post-MI. The granulation stage is characterized by a gradual increase of granulation tissue peaking during the second week and disappearing completely during the fourth week. Los was administered by gavage at a dose of 12.5 $mg \cdot kg^{-1} \cdot day^{-1}$.

Ventricular function experiments. At the end of the protocols, animals were anesthetized with 75 mg/kg ketamine and 0.75 mg/kg xylazine, as described above. Afterward, arterial blood pressure was recorded using a catheter placed inside the femoral artery (12).

Immediately afterward, animals were killed with an overdose of thiopental sodium. Subsequently, the thorax was opened, and hearts were rapidly excised and placed in a perfusion system according to the modified Langendorff technique. This procedure was completed in <1 min. Hearts were perfused with a Krebs-Henseleit buffer containing (in mM) 118.5 NaCl, 4.7 KCl, 24.8 $NaHCO_3$, 1.2 KH_2PO_4, 1.2 $MgSO_4$, 2.5 $CaCl_2$, and 10 glucose at pH 7.4 ± 1.4 and bubbled with 95% O_2-5% CO_2 at 37°C.

A latex balloon linked to a rigid polyethylene tube was placed into the left ventricular (LV) cavity and connected to a Deltram II pressure transducer (Utah Medical Systems) to allow measurement of LV pressure (in mmHg). This variable was recorded in real time using a computer with an analog-to-digital converter. A constant heart rate was maintained (175 beats/min) throughout the experiment with the use of two electrodes placed in the right atrium and at the base of the pulmonary artery.

After a 20-min period of stabilization, systolic and diastolic pressure-volume curves were generated. The latex balloon was filled with 0.1 ml of water at a time until the LV end-diastolic pressure (LVEDP) reached an approximate value of 40 mmHg. LVEDP values from each animal were fitted to an exponential function ($P = b \times e^{KV}$, where P is pressure, *b* is the initial value of P when volume (V) is zero, and K is the constant rate of exponetial growth) using a Deltagraph 7.0. This adjustment generated volumes at a given pressure. After this, average volumes for each group were obtained, and pressure-volume curves were generated. Ventricular systolic function was evaluated through the analysis of the relationship between LV developed pressure (LVDP) and LV end-diastolic volume.

Quantitative determination of infarct size. After functional determinations, hearts were arrested in diastole with 2 M KCl. The balloon was then refilled with water until it reached a final physiological pressure (~10 mmHg). Afterward, hearts were perfused with 10% formaldehyde (pH 7.2), allowing 5 min for fixation, and then remained in formaldehyde with the same volume for 72 h. Hearts were cut in slices from the apex to base. Slices from a middle section of the hearts were paraffin embedded, and 5-μm-thick sections were stained with hematoxylin and eosin (H&E) and Masson's trichrome. Slices stained with Masson's trichrome were scanned, and the following variables were calculated from planimetric measurements using Image Pro-Plus 6.0 software (Media Cybernetics, Silver Spring, MD): *1*) infarct size was calculated as the total length of the scar as a percentage of the total LV circumference, using the average of

endocardial and epicardial tracings; and *2*) the scar thinning ratio was calculated as the ratio between the thickness of the scar and the average thickness of the noninfarcted septum in the same slice.

Histomorphometric analysis. Hearts from each group at 35 and 56 days postsurgery were used for histological analysis (n = 4–5 hearts/group). After death, hearts were excised from the thorax and immersed in 10% formaldehyde for 72 h. Later, hearts were cut from the apex to base and embedded in paraffin, 5-μm serial cuts were made, and sections were stained with H&E and Picrosirius red. Thus, tissue modifications that could be caused by Langendorff perfusion were avoided.

Myocyte cross-sectional areas were determined on digitalized images of rhodamine-conjugated lectin-stained sections (WGA no. RL-1022, Vector Laboratories, Burlingame, CA) of paraffin-embedded samples. These digitalized images were obtained using a fluorescence microscope (Olympus BX61) attached to a digital camera and connected to a computer equipped with image-analysis software. Outlines of myocytes were traced, and cell areas were measured with Image Pro-Plus 6.0. At least 80 measurable cross sections of myocytes from the septum were routinely measured (7).

In slices stained with Picrosirius red, interstitial collagen deposition was also measured in the septum and scar using the image-analysis system described above. The percentage of collagen for each region was calculated by adding the areas corresponding to collagen and dividing by the addition of the areas corresponding to myocytes plus the areas of collagen tissue.

Measurement of infiltrating neutrophils, macrophages, and lymphocytes. Hearts from rabbits killed at 4, 35, and 56 days post-MI (n = 4–5 hearts/group) were used for the measurement of cellular inflammatory infiltrate in the infarct zone. After death, hearts were excised and histologically processed as mentioned above. H&E-stained tissue sections were obtained, and quantitative assessment of neutrophils, macrophages, and lymphocytes was carried out in randomly chosen high-power fields (HPFs; ×400) based on their morphological characteristics as previously described (5). To confirm these measurements, adjacent tissue sections were immunolabeled with the following antibodies: monoclonal mouse anti-rabbit RAM 11 (no. M-0633, DAKO Cytomation, Carpinteria, CA) and monoclonal mouse anti-human CD 45 RO (clone UCHL1, no. M-0742, DAKO Cytomation) (1) for macrophages and lymphocytes, respectively. The rabbit tonsil was used as a positive control for macrophages (18) and the rabbit lymph node for lymphocytes (4). Afterward, immunolabeling was detected with the use of a commercial kit (K0679, Universal LSAB). Images were captured using an Olympus microscope.

Temporal activation of the RAS post-MI in rabbits. Temporal activation of the RAS after MI was studied. Circulating and cardiac levels of ANG II as well as cardiac AT_1R expression were determined at 3 and 24 h and 4, 15, and 35 days of MI evolution (n = 4–5 hearts/group). Accordingly, after death, hearts from each set of animals were dissected, and the MI and non-MI zones from the LV were separated and immediately frozen in nitrogen for the measurement of ANG II levels by EIA and AT_1R expression by Western blot analysis.

Circulating and tissue ANG II assays by EIA. Plasma and cardiac ANG II levels were assessed using a commercial EIA kit (SPI-BIO Bertin, Montigny le Bretonneux, France) (13). Whole blood was collected in chilled EDTA-containing tubes, and plasma was separated by centrifugation at 3,000 *g* for 10 min at 4°C and stored at −70°C until processed. Frozen tissues from both MI and non-MI ventricular zones were placed into 0.1 mol/l acetic acid [1:10 (wt/vol)] containing EDTA (25 mM) and protease inhibitors and transferred to a boiling water bath for 10 min. After being cooled on ice, samples were homogenized and centrifuged at 13,000 *g* for 15 min at 4°C, and supernatants were separated.

Plasma and supernatants were passed through phenyl cartridges (Amprep minicolumns, Amersham Biosciences). The methanol elute was dried, reconstituted with EIA buffer, and assayed to detect ANG II by EIA according to the manufacturer's instructions. Absorbance at 405 nm was recorded, and ANG II concentrations were calculated from a standard curve generated for each experiment.

Tissue AT_1R assay by Western blot analysis. After death, hearts from each set of animals were dissected and cut in the middle to separate the apex from the base.

Tissues were homogenized in ice-cold 50 mM Tris·HCl buffer (pH 7.4) containing 5 mM EDTA, 150 mM NaCl, 0. 1% SDS, 1 mmol/l PMSF, 10 μg/ml aprotinin, and 2 μg/ml leupeptin and were centrifuged at 2,600 *g* for 5 min at 4°C. The resulting supernatant was further centrifuged at 40,000 *g* for 40 min at 4°C to obtain pellets (membrane fraction). Pellets were suspended in homogenization buffer, and the protein content was determined by the Bradford protein assay. Equal amount of proteins were subjected to 10% SDS-PAGE and transferred electrophoretically to polyvinylidene difluoride membranes with transfer buffer containing 25 mmol/l Tris, 192 mmol/l glycine, and 20% methanol. Nonspecific binding sites on the membrane were blocked by an incubation with 5% milk in Tris-buffered saline solution containing 0.1% Tween 20. Membranes were subsequently blotted with rabbit anti-AT_1R antibody (Santa Cruz Biotechnology) followed by an incubation with goat anti-rabbit IgGs coupled to horseradish peroxidase. Immunoreactive bands were visualized by chemioluminescence detection (ECL Plus reagent, Amersham) and quantified by densitometry. Protein loading in gels was evaluated by reblotting membranes with anti-actin antibody.

Statistical analysis. All values are expressed as means ± SE. Survival was analyzed using Kaplan-Meier analysis, and the log-rank test was used to evaluate for significant differences among groups. Pressure-volume curves were tested by two-way ANOVA for repeated measures followed by Bonferroni's test. One-way ANOVA followed by the Newman-Keuls post test was also used for comparing individual differences in arterial blood pressure and also for morphometric and histological measurements. $P < 0.05$ was considered statistically significant.

Table 1. *Blood pressure, heart and body weight, and infarct size*

	n	Body Weight, kg		Heart Weight/Body Weight, g/kg	Mean Arterial Blood Pressure, mmHg	Infarct Size, %
		Early	Late			
$Sham_{35}$	6	2.14±0.05	2.52±0.07	2.52±0.07	84±1,7	
MI_{35}	13	2.18±0.07	2.67±0.08	2.67±0.08	86±2,7	26.77±2.74
MI_{35} + $Los_{[0]}$	12	2.13±0.04	2.52±0.08	2.52±0.08	73±0,8*†	28.16±2.39
MI_{35} + $Los_{[15]}$	12	2.29±0.16	2.75±0.10	2.75±0.10	74±1,4*†	24.86±3.10
$Sham_{56}$	6	2.14±0.09	2.73±0.06	2.73±0.06	84±1,7	
MI_{56}	12	2.05±0.04	2.66±0.02	2.66±0.02	77±2,7‡	21.89±3.72
MI_{56} + $Los_{[15]}$	12	2.18±0.07	2.73±0.09	2.73±0.09	73±1,6‡	23.53±2.11

Values are means ± SE; n, no. of animals/group. Mean arterial blood pressure was measured at the end of the protocol. Animals were divided into the following groups: sham treatment of 35 days ($Sham_{35}$) or 56 days ($Sham_{56}$), untreated myocardial infaction (MI) of 35 days of evolution (MI_{35}), MI evolution of 35 days with losartan (Los) treatment from the beginning of the protocol until *day 35* (MI_{35} + $Los_{[0]}$), MI evolution of 35 days with Los treatment from *day 15* post-MI (MI_{35} + $Los_{[15]}$), untreated MI with 56 days of evolution (MI_{56}), MI evolution of 56 days with Los treatment from *day 15* post-MI (MI_{56} + $Los_{[15]}$). *$P < 0.05$ vs. the $Sham_{35}$ group; †$P < 0.05$ vs. the MI_{35} group; ‡$P < 0.05$ vs. the $Sham_{35}$ group.

RESULTS

Blood pressure, heart and body weight, and infarct size. Animal characteristics and arterial blood pressures are shown in Table 1. The body weight at the beginning of the protocol was similar in all groups. At the end of the experiment, body weights and heart weight-to-body weight ratios were similar between groups (Table 1).

At 35 days postsurgery, mean arterial blood pressure was reduced in both Los-treated groups ($P < 0.05$ vs. untreated groups). At 56 days post-MI, mean arterial blood pressure was reduced in both infarcted and noninfarcted groups, and there were no significant differences between both MI groups (Table 1). Infarct sizes were similar among groups (Table 1).

Survival. Survival rates are shown in Fig. 2. All animals in the sham group completed the protocol. The survival rate was significantly lower in MI_{35} and MI_{35} + $Los_{[0]}$ groups ($P = 0.019$ and $P = 0.004$ vs. the sham group). No differences were found in the MI_{35} + $Los_{[15]}$ and MI_{35} + $Los_{[0-4]}$ groups. At 56 days, the survival rate was reduced in the MI_{56} group ($P = 0.017$ vs. the sham group). This reduction was slightly attenuated in the MI_{56} + $Los_{[15]}$ group without achieving statistical significance (Fig. 2).

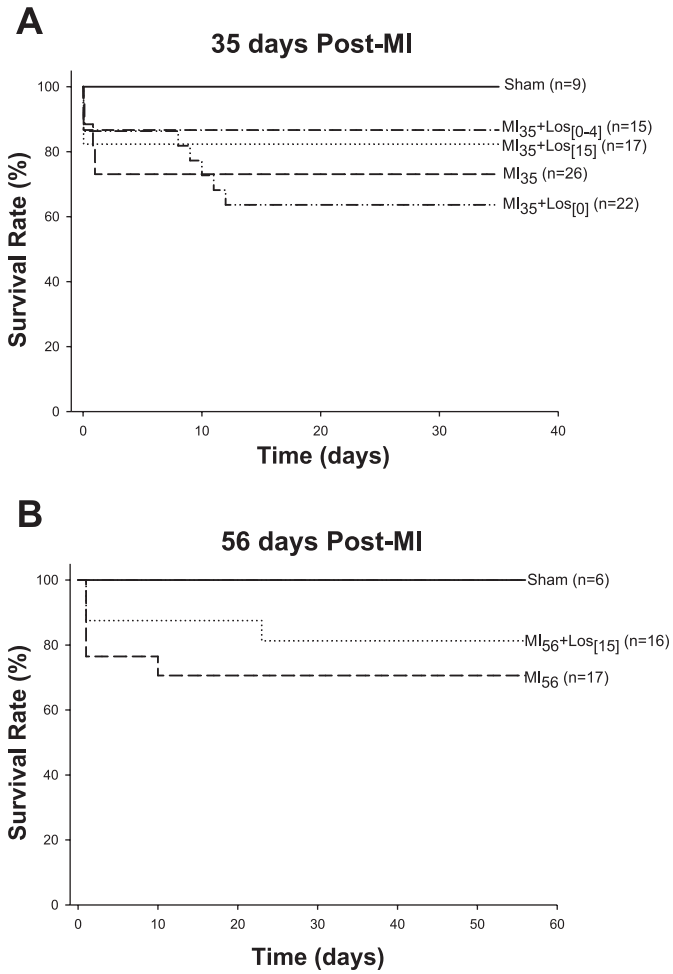

Fig. 2. Survival curves at 35 days (*A*) and 56 days (*B*). The MI_{35} and MI_{35} + $Los_{[0]}$ groups had significantly reduced survival compared with the sham group ($P = 0.019$ and 0.004, respectively). No significantly differences were found in the MI_{35} + $Los_{[15]}$ and MI_{35} + $Los_{[0-4]}$ groups compared with the sham, MI_{35}, and MI_{35} + $Los_{[0]}$ groups. At 56 days in untreated animals, there was a reduction in the survival rate ($P = 0.017$ vs. the sham group). No significant differences were found in animals treated from *day 15* post-MI with respect to animals in the sham and MI_{56} groups.

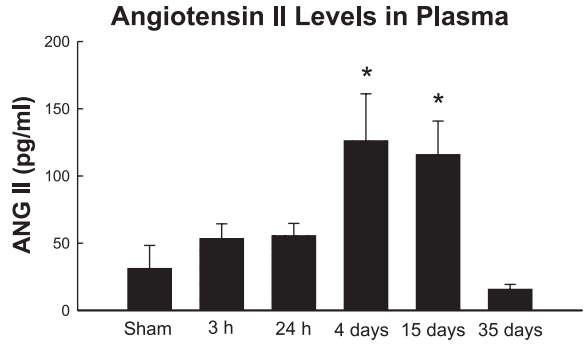

Fig. 3. ANG II levels in plasma from 3 h to 35 days post-MI were measured by ELISA as described in METHODS. ANG II increased in plasma at 4 and 15 days post-MI and then declined to control values at 35 days. *$P < 0.05$ vs. the sham group.

Plasma ANG II levels. As shows in Fig. 3, circulating ANG II levels were significantly increased at 4 and 15 days post-MI and then decreased, reaching control values at 35 days.

Temporal evolution of AT$_1$R expression and ANG II content. Figure 4 shows AT$_1$R expression in non-MI and MI areas of

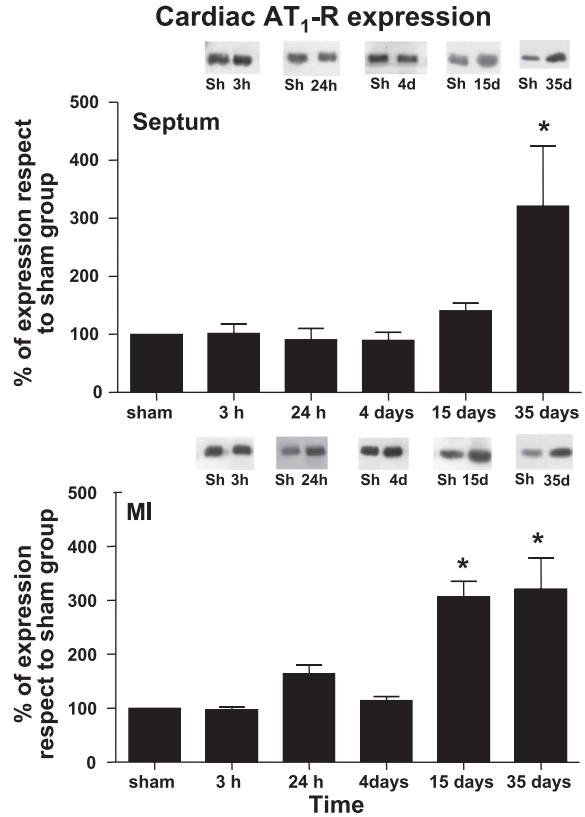

Fig. 4. ANG II type 1 receptor (AT$_1$R) expression in noninfarcted (septum; *top*) and infarcted (*bottom*) left ventricles (LVs). AT$_1$R expression was measured by Western blot analysis (*insets*) as described in METHODS and is expressed as the percentage of the response detected at 3 h and 24 h and 4, 15, and 35 days with respect to the corresponding sham (Sh) animals. Each time incubation period had its own control, although only one control (sham) result is shown. Each bar represents the mean ± SE of 3 determinations from 5 separate animals. *$P < 0.01$ vs. the sham group.

rabbit hearts at 3 h and 1, 4, 15, and 35 days. No differences in the expression of AT$_1$R were found between non-MI and MI zones during the first 4 days postligature. At 15 and 35 days post-MI, AT$_1$R expression was significantly increased in the MI zone. In the non-MI zone, this increase reached statistical significance at 35 days post-MI.

Figure 5 shows the time course of ANG II levels in non-MI (septum) and MI zones. ANG II content was increased in the non-MI myocardium from 3 h up to 4 days but just reached significance ($P < 0.05$) at 24 h post-MI, whereas in the MI zone, ANG II levels were significantly augmented at 4 days post-MI and progressively decreased until 35 days postligature (Fig. 5).

Pressure-volume curves. Figure 6*A* shows systolic pressure-volume curves in 35-day MI groups. MI caused a significant reduction in LVDP in untreated animals and those treated with Los from the beginning of the infarction ($P < 0.05$ vs. the sham group), whereas in the MI$_{35}$ + Los$_{[15]}$ group, the decrease of myocardial contractility was attenuated. Figure 6*B* shows the systolic pressure-volume relation at 56 days after surgery. In the MI$_{56}$ group, there was a significant decrease in systolic function ($P < 0.05$ vs. the sham group). In addition, in the MI$_{56}$ + Los$_{[15]}$ group, there was a significant decrease in systolic function ($P <$ 0.05 vs. the sham group).

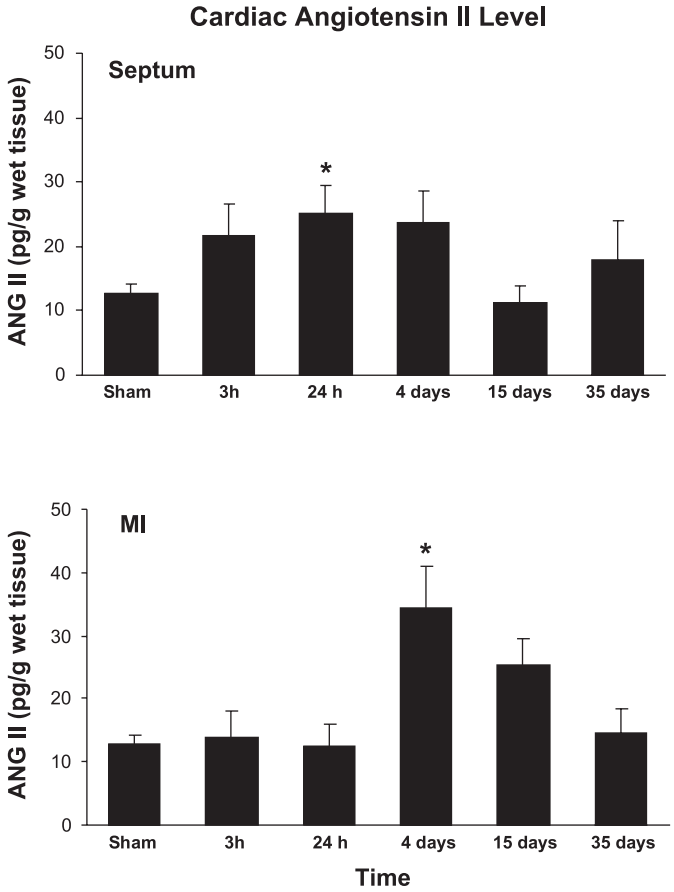

Fig. 5. ANG II levels in the noninfarcted (septum; *top*) and infarcted (*bottom*) myocardium. Bars represent ANG II tisular content (in pg/g wet tissue) at 3 h and 24 h and 4, 15, and 35 days in sham and MI groups. ANG II increased in the non-MI zone from 3 h to 4 days post-MI, although it only reached statistical significantce at 24 h; afterward, ANG II levels declined to control values at 15 and 35 days. In the MI zone, ANG II levels increased at 4 days and then progressively decreased until 35 days postligature. *$P < 0.05$ vs. the sham group.

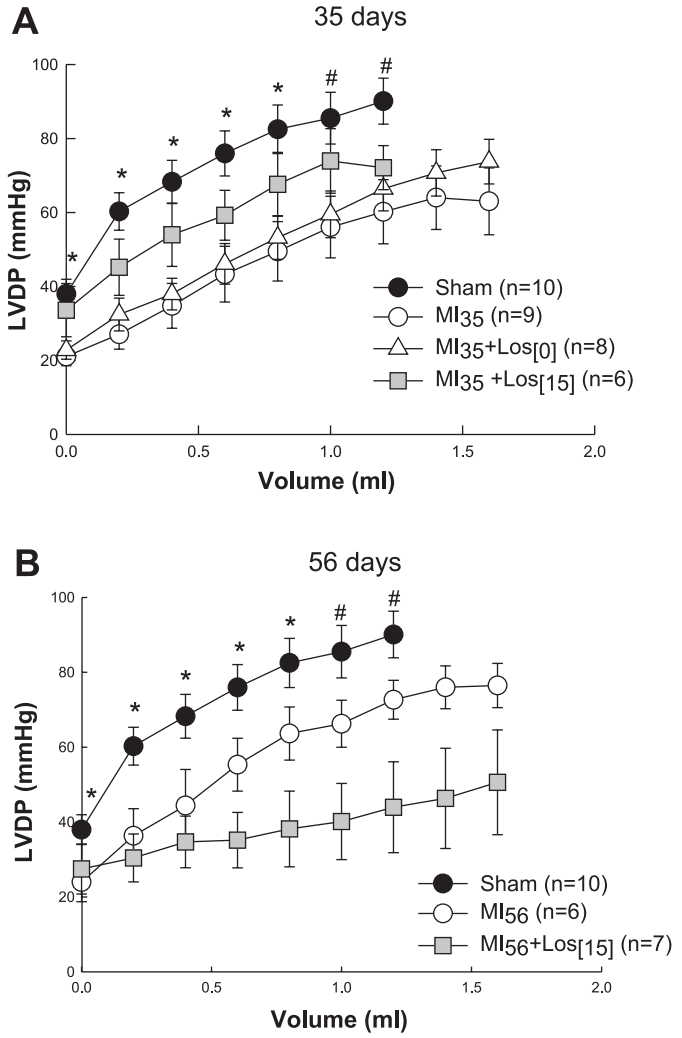

Fig. 6. Systolic pressure-volume curves. *A*: groups at 35 days postsurgery; *B*: groups at 56 days postsurgery. At 35 days postsurgery, both the MI group and the MI group treated with Los from the beginning of the protocol showed reduced contractile function compared with either sham animals or with animals treated with Los from *day 15*. At 56 days, the MI group showed in reduced contractile function compared with sham animals, and in the group treated with Los, the systolic ventricular function was even more reduced. LVDP, LV developed pressure. *$P < 0.05$ vs. MI and MI + Los$_{[15]}$ groups; #$P < 0.05$ vs. MI groups.

Figure 7, *A* and *B*, shows diastolic pressure-volume curves at 35 and 56 days after surgery. In the MI$_{35}$, MI$_{35}$ + Los$_{[0]}$, and MI$_{35}$ + Los$_{[15]}$ groups, there was an increase in the LV cavity size, as evidenced by a shift to the right in the diastolic pressure-volume relation. The shift of the curve in the MI$_{35}$ + Los$_{[15]}$ group was similar to that in the MI$_{35}$ group ($P < 0.05$ vs. the sham group), whereas in the MI$_{35}$+Los$_{[0]}$ group, the shift of the pressure-volume relation to the right was even greater, reaching statistical significance with the other three groups.

At 56 days, there was also a significant shift to the right in the pressure-volume curve in the MI$_{56}$ group ($P < 0.05$ vs. the sham group). At this time, the pressure-volume curve in the MI$_{56}$ + Los$_{[15]}$ group, like in the MI$_{35}$ + Los$_{[0]}$ group, was

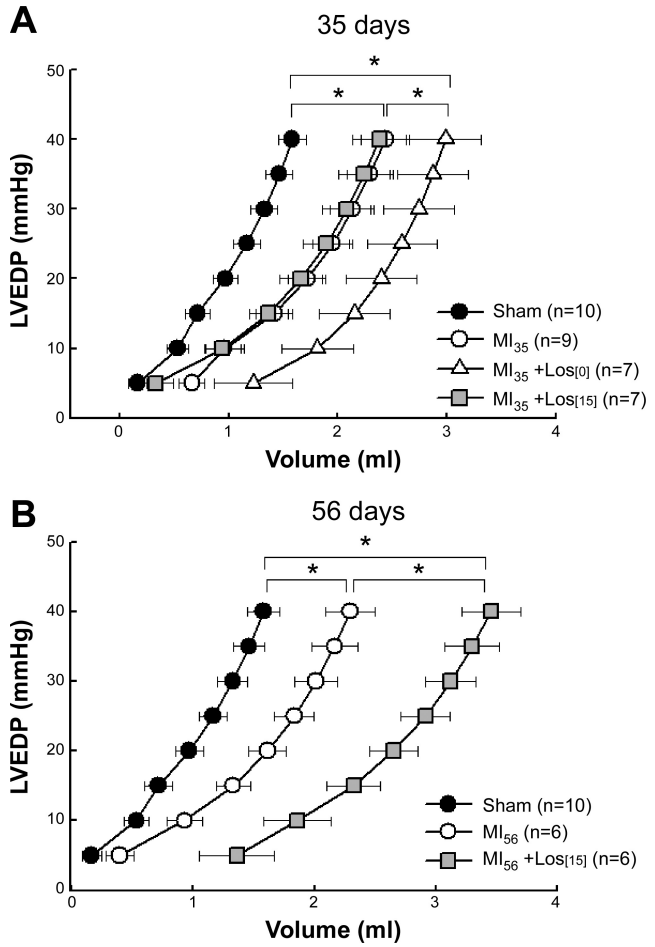

Fig. 7. Diastolic pressure-volume curves in animals at 35 days (*A*) and 56 days (*B*) postsurgery. The treatment with Los from the beginning of MI resulted in a shift of pressure-volume curves to the right compared with the sham, MI_{35}, and MI_{35} + $Los_{[15]}$ groups. At this time, the curves of MI hearts in animals treated with Los from *day 15* were similar to untreated MI animals ($P < 0.05$ vs. the sham group). At 56 days postsurgery, untreated MI animals showed a shift of pressure-volume curves to the right, whereas in the MI_{56} + $Los_{[15]}$ group, this shift was even more to the right and similar to that observed in the MI_{35} + $Los_{[0]}$ group. LVEDP, LV end-diastolic pressure. *$P < 0.05$.

shifted even further to the right, showing increased ventricular dilation compared with the MI_{56} group ($P < 0.05$ vs. the MI_{56} group).

Histomorphometric analysis. To elucidate the possible mechanisms underlying the cardiac function impairment, we analyzed the histomorphometric and histological characteristics of hearts in the infarct and remote zones. Figures 8 and 9 show morphometric measurements obtained from the septum and infarcted zones at 35 and 56 days post-MI, respectively. The myocyte cross-sectional area in the septum from a middle section of the heart was increased in both untreated MI groups ($P < 0.05$ vs. the sham group) but was significantly attenuated in all Los-treated groups, with this attenuation being greater in those groups treated for a longer time (Fig. 8). Remodeling was also assessed by the scar thinning ratio from middle heart slices stained with Masson's trichrome. As shown in Fig. 9, the administration of Los from the beginning of MI reduced the scar thinning ratio ($P < 0.05$ vs. the MI_{35} group). However, this was not observed in animals treated from *days 15* to *35* and *56* (MI_{35} + $Los_{[15]}$ and MI_{56} + $Los_{[15]}$ groups).

Collagen content in the septum (Fig. 10) was increased in both untreated MI groups ($P < 0.05$ vs. the sham group). This increase was significantly attenuated in all Los-treated groups. The increased collagen content in the scar caused by the infarction was reduced by Los treatment from *day 0* but not

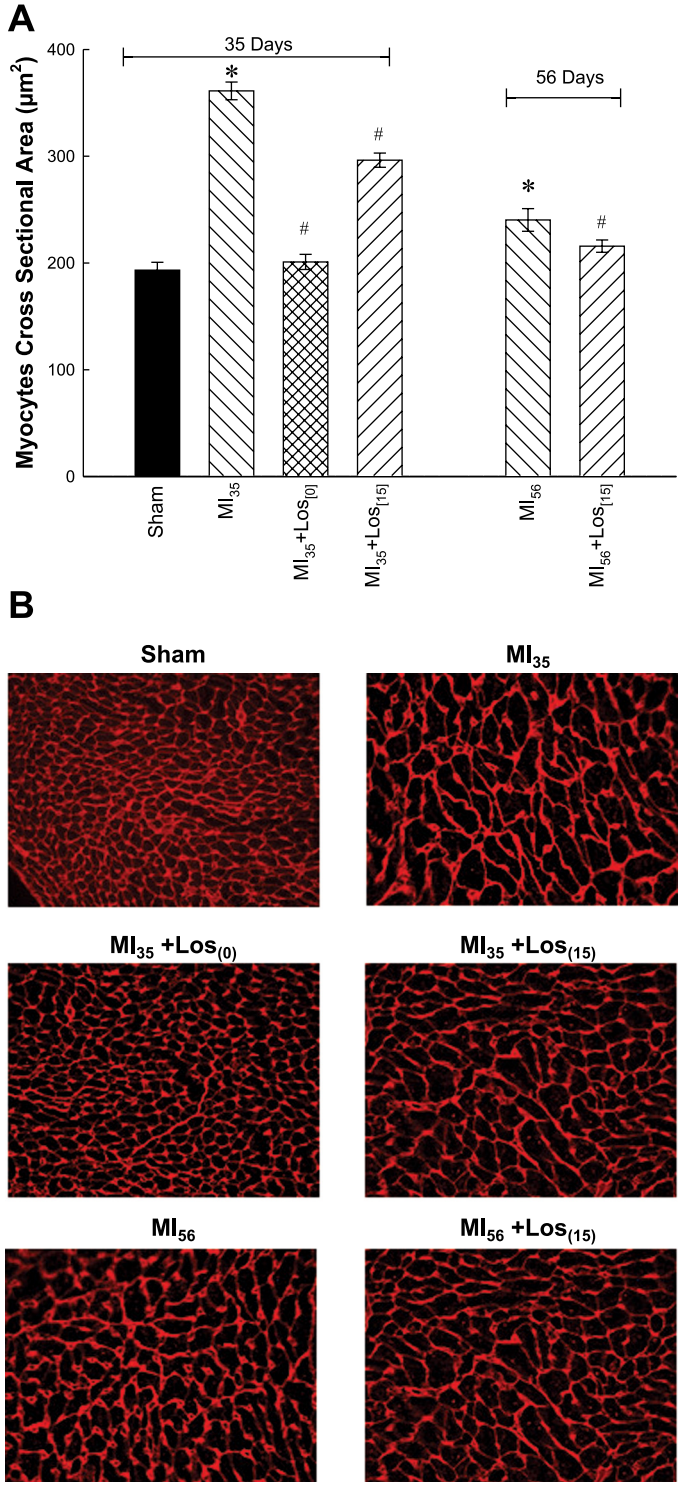

Fig. 8. *A*: myocyte cross-sectional areas were increased in MI groups and reduced in all Los-treated groups. *B*: representative rhodamine-conjugated lectin-stained sections for all groups. Magnification: ×400. *$P < 0.05$ vs. the sham group; #$P < 0.05$ vs. MI groups.

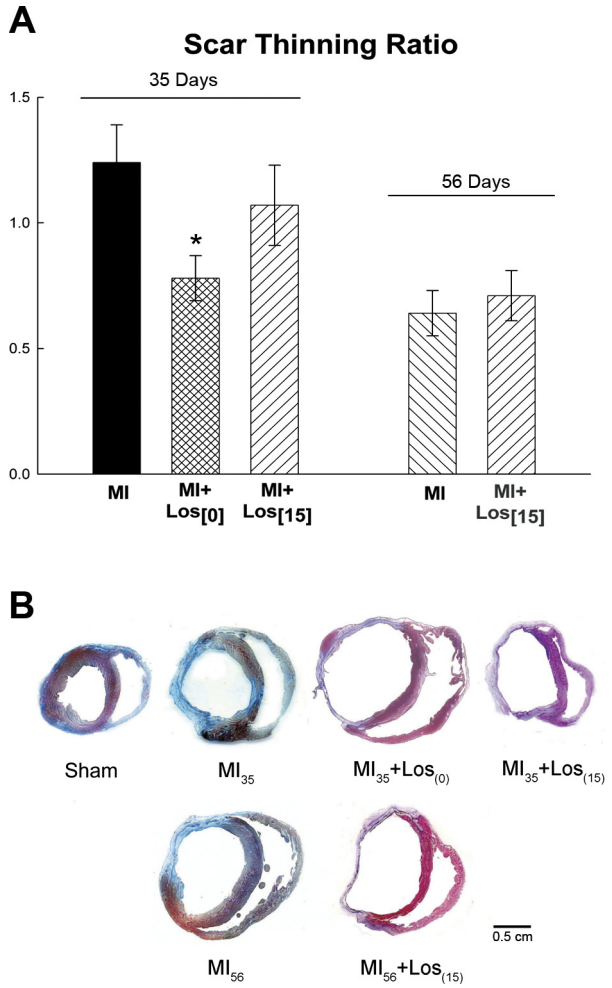

Fig. 9. *A*: scar thinning ratios in the groups of animals at 35 and 56 days postsurgery. There was a reduction in the scar thinning ratio only in the group treated with Los from the beginning of the protocol. At 56 days postsurgery, the thinning ratio was reduced in the untreated MI group, and no differences were found compared with the group treated with Los. *B*: representative Masson's trichrome-stained sections from all infarcted groups. Note the increase in ventricular dilation, the thinning of the scar, and the reduction of the septum width in both groups treated with Los for the longer time. Since the infarct size was calculated with all the slices of each heart, these slices do not represent the infarct size of each group. *$P < 0.05$ vs. the MI group.

from *day 15* in the MI_{35} group. In contrast, the scar collagen content was reduced when Los was administered from *day 15* in the MI_{56} group (Fig. 11).

Inflammatory cellular infiltrate. Figure 12, *A–C*, shows the quantitative determination of inflammatory cellular components in the early and chronic phase of infarction in untreated and Los-treated animals. Treatment with Los significantly reduced neutrophil, macrophage (RAM 11-positive cells), and lymphocyte (CD45 RO-positive lymphocytes) infiltration at 4 days post-MI in the MI zone, indicating a clear anti-inflammatory effect of Los on MI wound healing (Fig. 12, *A*, *top*, and *D* and *E*). On the other hand, at 35 days postligature, CD45 RO-positive lymphocytes and RAM 11-positive macrophages were still detected in both Los-treated groups ($P < 0.05$ vs. the MI_{35} group; Fig. 12, *B*, *D*, and *E*) suggesting a delay in the wound healing. No differences were found at 56 days (Fig. 12*C*).

DISCUSSION

In the present study, we found that cardiac and circulating ANG II levels were increased in rabbits within 4 days post-MI while AT_1R expression was upregulated after 15 days. In addition, Los treatment significantly reduced inflammatory infiltrate in the early stage of MI (MI_4 + $Los_{[0]}$) and maintained the presence of RAM 11-positive macrophages and CD45 RO-positive lymphocytes in the scar tissue at 35 days (MI_{35} + $Los_{[0]}$ and MI_{35} + $Los_{[15]}$). Furthermore, long-term therapy with Los (MI_{35} + $Los_{[0]}$ and MI_{56} + $Los_{[15]}$) unfavorably modified ventricular function and remodeling and tended to reduce the survival rate when treatment was started at the beginning of the infarction. These data, together with the reduction of the scar collagen content observed in animals treated from the beginning of MI, reinforce the evidence that AT_1R blockade affects the dynamics of the healing process as a mechanism likely contributing to the effect of global remodeling (21). In contrast, midterm therapy with Los (MI_{35}+$Los_{[15]}$) did not cause a shift in the diastolic pressure-volume curve compared with MI, attenuated the impairment of LVDP and did not modify the scar collagen content. Finally, we observed that midterm and early short-term therapy with los (MI_{35} + $Los_{[15]}$ and MI_{35} + $Los_{[0-4]}$) reduced mortality at 35 days post-MI.

Previous studies (2, 17, 31, 36) performed in rats have reported 4.2-fold increase in ANG II levels in the MI zone at 3 wk post-MI, whereas no changes were found in the remote zones (43). On the other hand, Van Kats et al. (39) showed no changes in temporal ANG II plasma and cardiac levels from 1 to 6 wk after MI in pigs. In our study, plasma ANG II levels peaked at 4 and 15 days post-MI and then declined. In addition, cardiac ANG II levels were increased earlier in the septum than in the MI zone, suggesting that the temporal influence of ANG II on the remodeling of the remote zone may be independent from that observed in the MI zone. Furthermore, we showed that the expression of AT_1R was upregulated after 15 days post-MI. Thus, our results may compliment and extend previous findings from Gallagher et al. (11), and they also confirm

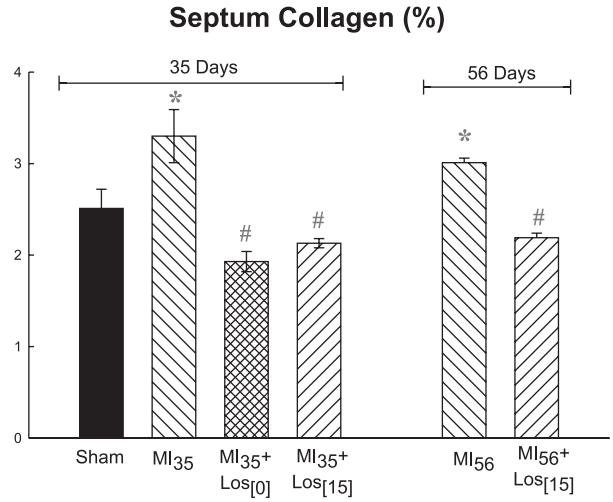

Fig. 10. Collagen content in the septum was increased in both untreated MI groups. The administration of Los significantly reduced the septum collagen content in all treated groups. *$P < 0.05$ vs. the sham group; #$P < 0.05$ vs. MI groups.

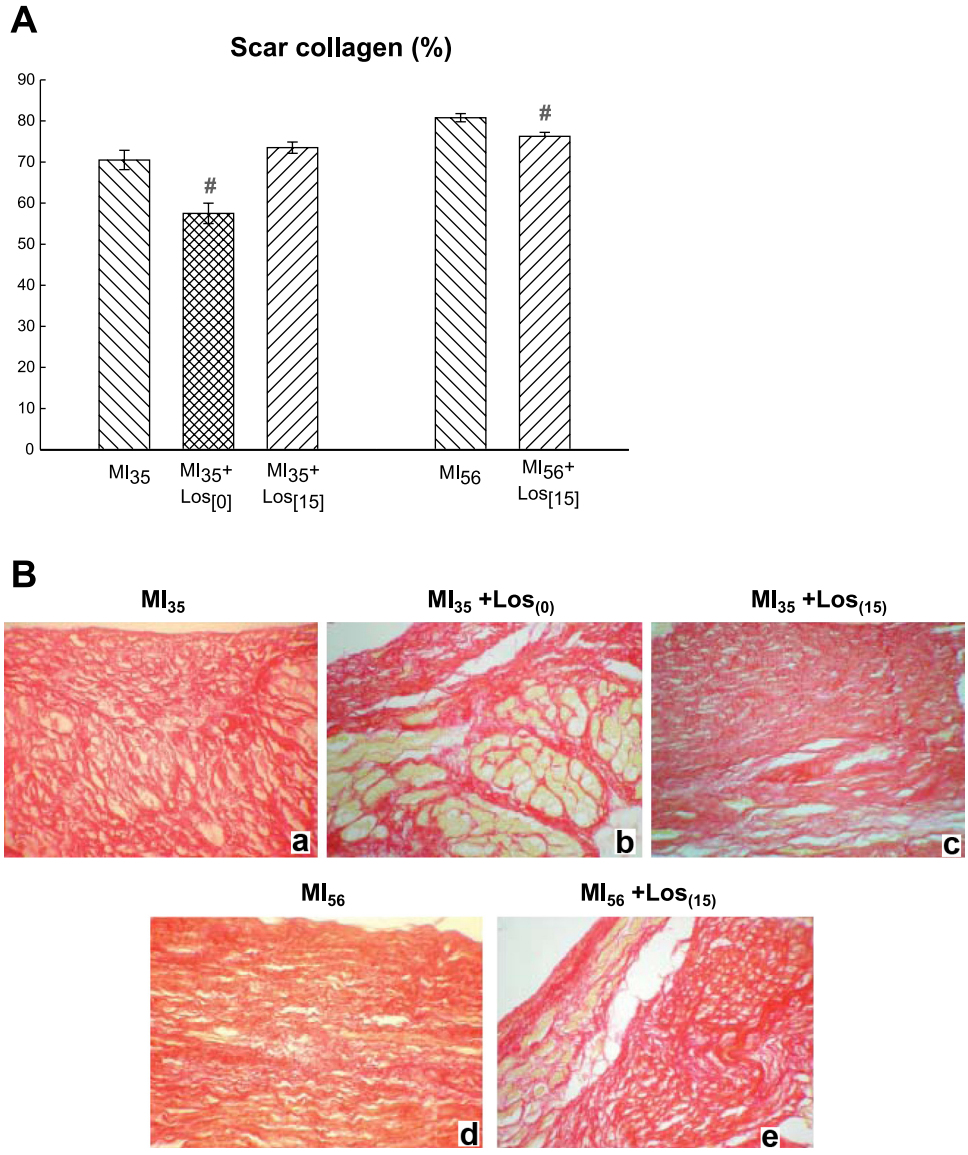

Fig. 11. *A*: collagen content measured in the scar. Collagen content was significantly reduced in groups treated for a long period of time (MI_{35} + $Los_{[0]}$ and MI_{56} + $Los_{[15]}$). This reduction was not observed in animals treated for 20 days (MI_{35} + $Los_{[15]}$). *B*: representative Picrosirius red-stained sections of the infarcted area in all MI groups. Note the reduction in the scar collagen content in the MI_{35} + $Los_{[0]}$ and MI_{56} + $Los_{[15]}$ groups. This reduction was not observed in the MI_{35} + $Los_{[15]}$ group. #$P <$ 0.05 vs. MI groups.

that this activation differs from that previously described in other species. In our study, most of rabbits with MI died within the first 2 wk, in accordance with the increase in ANG II levels in the plasma and MI zone. Therefore, the fact that early long-term treatment with Los (MI_{35}+$Los_{[0]}$) increased mortality within this period of time in which plasma and infarct zone ANG II levels were increased and the fact that this was not observed in any other treated groups (MI_{35} + $Los_{[0\text{-}4]}$, MI_{35} + $Los_{[15]}$, and MI_{56} + $Los_{[15]}$) suggest that ANG II blockade with Los in MI rabbits is detrimental for survival. This first conclusion may be strengthened by the fact that early short-term treatment with Los significantly reduced neutrophils, RAM 11-positive macrophages, and CD45 RO-positive lymphocytes at 4 days post-MI, whereas long-term therapy delayed the healing process, as determined by the persistency of these inflammatory cells and the reduction of collagen content at 35 days. In contrast with results reported in other species (16, 21, 27, 31, 37), long-term therapy increased the dilation and

Fig. 12. *A*: neutrophil, RAM 11-positive macrophage, and CD45 RO-positive lymphocyte infiltrates at the infarct zone in untreated and Los-treated animals at 4 days post-MI. The early administration of Los significantly reduced cellular inflammatory infiltrate at the beginning of MI. *B*: CD45 RO-positive lymphocytes and RAM 11-positive macrophages were increased at 35 days in Los-treated animals. *C*: no differences were found at 56 days. *D*: representative images of RAM 11-immunostained sections (original magnification: ×400) of the infarct zone in untreated and Los-treated animals at 4 and 35 days post-MI. Treatment with Los clearly reduced macrophages (arrows) at the early stage and preserved them at 35 days. Microphotographs of animals at 56 days are not shown because no differences were found between Los-treated and untreated animals. The *insets* (original magnification: ×1,000) show typical RAM 11-positive labeling for macrophages. Note the microphotograph of the rabbit tonsil, which used as a positive control for macrophages. *E*: representative images of CD45 RO-immunostained sections (original magnification: ×400) of the infarct zone in untreated and Los-treated animals at 4 and 35 days post-MI. Treatment with Los clearly reduced CD45 RO-positive lymphocytes (arrows) and preserved them at 35 days. Microphotographs of animals at 56 days are not shown because no differences were found between Los-treated and untreated animals. The *insets* (original magnification: ×1,000) show typical CD45 RO immunohistochemical labeling for CD45 RO-positive lymphocytes. Note the microphotograph of the rabbit lymph node, which was used as a positive control for lymphocytes. *$P <$ 0.05 vs. MI.

reduced the scar collagen content at 35 and 56 days post-MI. In animals treated with Los from the beginning of MI, we also found a significant reduction in the scar thickness at 35 days. Even though no significant difference in the scar thickness was found at 56 days between groups, it is important to note that this ratio was similar in the MI_{56} + $Los_{[15]}$ group compared with the MI_{35} + $Los_{[0]}$ group (Fig. 9). Changes observed in function and remodeling after treatment with Los compared with untreated animals clearly confirm that Los administration was effective in modifying mortality and the remodeling process.

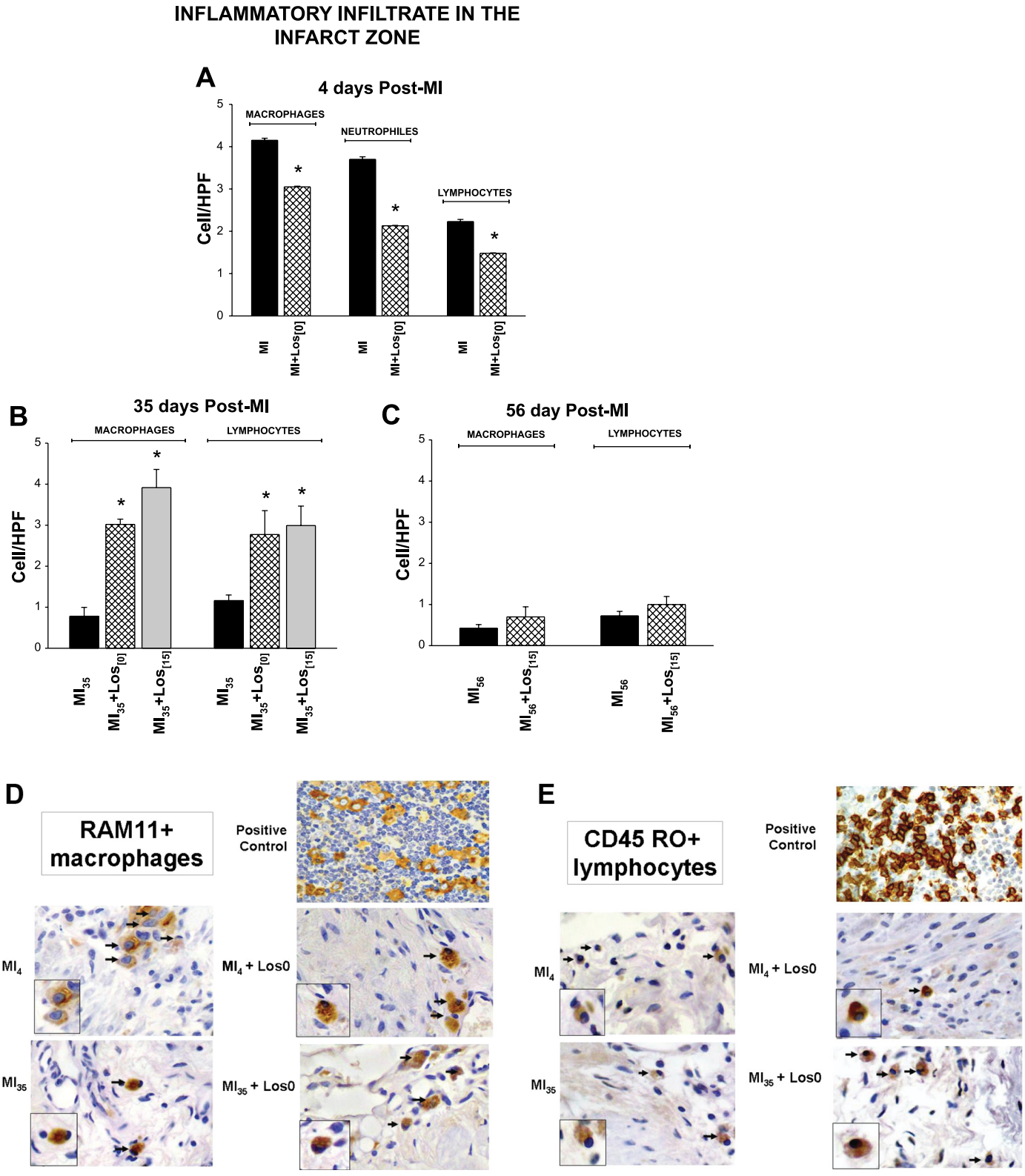

Another important issue to be considered, and closely related to the previous topic, is the effect of RAS blockade on inflammatory infiltrate and the healing process after MI (21, 32). In our previous study (12), we found that early long-term therapy with Los in rabbits with MI unfavorably modified ventricular remodeling. Recently, Li et al. (21) reported a delay in the wound healing dynamics and lower collagen deposition in AT_1R knockout mice with MI. However, an increased infarct wall thickness and a reduced cavity size at 4 wk were described. In this sense, this is the first study in rabbits adding relevant information concerning the importance of considering the time and duration of AT_1R blockade to determine the evolution of remodeling.

According to our results, in long-term-treated groups, it is possible to speculate that the inflammatory cells still detected in the MI zone and the lower scar collagen deposition might have weakened the scar, increasing its distensibility (3, 14, 19), and these factors have chronically determined the degree of dilation and ventricular performance (14, 35). Additionally, an unbalance in the ratio of matrix metalloproteinase (MMP) and its inhibitors [tissue inhibitors of metalloproteinase (TIMPs)] could also participate in the delay of the healing process. We have not studied the effect of Los on MMP expression or activity; however, other studies (40, 42) have shown that AT_1R blockers can modify the balance between MMPs and TIMPs. These facts may explain, in some cases, the reason why AT_1R blockers failed to reduce the dilation and progression to heart failure (15, 37, 41). In this sense, Zdrojewsky et al. (45) showed in rats that chronic administration of quinapril reduced the scar collagen content and modified its structure. Interestingly, in that study, no change in ventricular dilation was observed. Another important issue to be considered is the effect of Los on the noninfarcted myocardium. The sustained volume overload increases parietal stress and myocyte growth, leading to compensatory hypertrophy and fibrosis in the septum (26). In our study, Los significantly reduced the myocyte cross-sectional area and fibrosis in the septum. The reduction of interstitial collagen was shown to diminish myocardial stiffness (38); this change can determine the ventricular dilation and shift the tension-length curve to the right (9, 24). Therefore, in our animals, it should be reasonable to believe that in these rabbits, the reduction of myocyte hypertrophy in the septum in association with the lower collagen content in the scar and remote zones may have contributed to exacerbate the observed ventricular dilation and systolic dysfunction observed. The fact that all treated animals reached the same mean arterial blood pressure at the end of the protocol suggests that the differences in remodeling due to Los treatment could not be attributed to changes in the mean arterial blood pressure. Consequently, taken together, these results suggest that adverse ventricular remodeling observed in long-term-treated rabbits with MI should not be unexpected.

The beneficial effects of AT_1R blockers have been mainly attributed to their capacity to reduce ventricular dilation (16), hypertrophy (27), and fibrosis (27, 38), thus contributing to the improvement of ventricular performance. According to our findings, significant healing defects might explain the accentuated adverse remodeling and may be closely related to the therapeutic design. Consequently, one important issue to be considered is the different windows for the initiation of therapy with AT_1R blockers and their effect on the healing process. However, despite the importance of this topic, there are few studies focusing on this issue, and they have shown controversial results (30, 33, 41) This fact could be clinically relevant in the treatment of patients with MI and may also explain several discrepancies concerning its beneficial effects. Clinical trials, such as the Optimal Trial in Myocardial Infarction with Angiotensin II Antagonist Losartan (8), Valsartan in Acute Myocardial Infarction Trial (28), and Losartan Heart Failure Survival Trial (29), have shown that AT_1R blockers reduced the morbidity/mortality rate and are well tolerated in patients with MI (34). In patients with heart failure who do not have markedly altered cardiac contractility, AT_1R blockers appears to have no clinical advantages over placebo treatment (23, 44). Additionally, in some of these trials, mortality was higher with AT_1R blockers over placebo treatment, among patients who had already taken a β-blocker (6).

In summary, the administration of Los to rabbits with MI reduced the survival and unfavorably modified the ventricular remodeling depending on the duration rather than on the onset of treatment. Our data strongly suggest that the delay in wound healing with the reduction of scar collagen content and the scar thinning ratio, in association with the reduction in the myocyte cross-sectional area and on interstitial collagen in the non-MI zone, could be responsible for this unfavorable remodeling, as determined by the increase in ventricular dilation and lower systolic performance. With midterm therapy, starting on *day 15*, no reduction in the scar collagen content was observed and the fall in contractility and dilation was attenuated. An important finding was that the temporal activation of the RAS, as determined by ANG II plasma and tissue levels as well as AT_1R expression, in rabbits is different from other species. Further experiments have to be done to elucidate other possible mechanisms by which Los produced unfavorable remodeling in rabbits.

ACKNOWLEDGMENTS

The authors thank Dr. Nidia Basso for critical reading of the manuscript. The technical assistance of Ana Chiaro is also gratefully acknowledged.

GRANTS

This work was supported by National Agency of Scientific and Technological Promotion Grants PICT 05-13069 and PICT 05-22037, National Council of Scientific and Technological Research Grant PIP 5820, and Department of Science of Technology of the University of Buenos Aires Grants M023 and M609. G. E. González, M. M. Gironacci, and R. J. Gelpi are Members of the National Council of Scientific and Technological Research (CONICET) of Argentina, S. Cavallero is a Postdoctoral Fellow of CONICET, and L. Wilensky is a Doctoral Fellow of CONICET. J. Palleiro is a Doctoral Fellow of the School of Medicine of the University of Buenos Aires, and I. M. Seropian is an Undergraduate Fellow of the University of Buenos Aires.

REFERENCES

1. **Behr-Roussel D, Rupin A, Simonet S, Bonhomme E, Coumailleau S, Cordi A, Serkiz B, Fabiani JN, Verbeuren TJ.** Effect of chronic treatment with the inducible nitric oxide synthase inhibitor *N*-iminoethyl-L-lysine or with L-arginine on progression of coronary and aortic atherosclerosis in hypercholesterolemic rabbits. *Circulation* 102: 1033–1038, 2000.
2. **Berthonneche C, Sulpice T, Tanguy S, O'Connor S, Herbert JM, Janiak P, de Leiris J, Boucher F.** AT_1 receptor blockade prevents cardiac dysfunction after myocardial infarction in rats. *Cardiovasc Drugs Ther* 19: 251–259, 2005.
3. **Bogen DK, Rabinowitz SA, Needleman A, McMahon TA, Abelmann WH.** An analysis of the mechanical disadvantage of myocardial infarction in the canine left ventricle. *Circ Res* 47: 728–741, 1980.
4. **Brown TJ, Crawford SE, Cornwall ML, Garcia F, Shulman ST, Rowley AH.** CD8 T lymphocytes and macrophages infiltrate coronary

artery aneurysms in acute Kawasaki disease. *J Infect Dis* 184: 940–943, 2001.

5. **Cavasin MA, Tao Z, Menon S, Yang XP.** Gender differences in cardiac function during early remodeling after acute myocardial infarction in mice. *Life Sci* 75: 2181–2192, 2004.
6. **Cohn JN, Tognoni G.** A randomized trial of the angiotensin-receptor blocker valsartan in chronic heart failure. *N Engl J Med* 345: 1667–1675, 2001.
7. **Depre C, Wang Q, Yan L, Hedhli N, Peter P, Chen L, Hong C, Hittinger L, Ghaleb B, Sadoshima J, Vatner DE, Vatner SF, Madura K.** Activation of the cardiac proteasome during pressure overload promotes ventricular hypertrophy. *Circulation* 114: 1821–1828, 2006.
8. **Dickstein K, Kjekshus J.** Effects of losartan and captopril on mortality and morbidity in high-risk patients after acute myocardial infarction: the OPTIMAAL randomised trial. Optimal Trial in Myocardial Infarction with Angiotensin II Antagonist Losartan. *Lancet* 360: 752–760, 2002.
9. **Diez J, Querejeta R, Lopez B, Gonzalez A, Larman M, Martinez Ubago JL.** Losartan-dependent regression of myocardial fibrosis is associated with reduction of left ventricular chamber stiffness in hypertensive patients. *Circulation* 105: 2512–2517, 2002.
10. **Frigerio M, Roubina E.** Drugs for left ventricular remodeling in heart failure. *Am J Cardiol* 96: 10L–18L, 2005.
11. **Gallagher AM, Bahnson TD, Yu H, Kim NN, Printz MP.** Species variability in angiotensin receptor expression by cultured cardiac fibroblasts and the infarcted heart. *Am J Physiol Heart Circ Physiol* 274: H801–H809, 1998.
12. **Gonzalez GE, Palleiro J, Monroy S, Perez S, Rodriguez M, Masucci A, Gelpi RJ, Morales C.** Effects of the early administration of losartan on the functional and morphological aspects of postmyocardial infarction ventricular remodeling in rabbits. *Cardiovasc Pathol* 14: 88–95, 2005.
13. **Graham HK, Trafford AW.** Spatial disruption and enhanced degradation of collagen with the transition from compensated ventricular hypertrophy to symptomatic congestive heart failure. *Am J Physiol Heart Circ Physiol* 292: H1364–H1372, 2007.
14. **Holmes JW, Borg TK, Covell JW.** Structure and mechanics of healing myocardial infarcts. *Annu Rev Biomed Eng* 7: 223–253, 2005.
15. **Hu K, Gaudron P, Anders HJ, Weidemann F, Turschner O, Nahrendorf M, Ertl G.** Chronic effects of early started angiotensin converting enzyme inhibition and angiotensin AT_1-receptor subtype blockade in rats with myocardial infarction: role of bradykinin. *Cardiovasc Res* 39: 401–412, 1998.
16. **Jain M, Liao R, Ngoy S, Whittaker P, Apstein CS, Eberli FR.** Angiotensin II receptor blockade attenuates the deleterious effects of exercise training on post-MI ventricular remodelling in rats. *Cardiovasc Res* 46: 66–72, 2000.
17. **Jones ES, Black MJ, Widdop RE.** Angiotensin AT_2 receptor contributes to cardiovascular remodelling of aged rats during chronic AT_1 receptor blockade. *J Mol Cell Cardiol* 37: 1023–1030, 2004.
18. **Knoess M, Krukemeyer MG, Kriegsmann J, Thabe H, Otto M, Krenn V.** Colocalization of C4d deposits/CD68+ macrophages in rheumatoid nodule and granuloma annulare: immunohistochemical evidence of a complement-mediated mechanism in fibrinoid necrosis. *Pathol Res Pract* 204: 373–378, 2008.
19. **Laird JD, Vellekoop HP.** The course of passive elasticity of myocardial tissue following experimental infarction in rabbits and its relation to mechanical dysfunction. *Circ Res* 41: 715–721, 1977.
20. **Leite-Moreira AF, Castro-Chaves P, Pimentel-Nunes P, Lima-Carneiro A, Guerra MS, Soares JB, Ferreira-Martins J.** Angiotensin II acutely decreases myocardial stiffness: a novel AT_1, PKC and Na^+/H^+ exchanger-mediated effect. *Br J Pharmacol* 147: 690–697, 2006.
21. **Li Y, Takemura G, Okada H, Miyata S, Kanamori H, Maruyama R, Esaki M, Li L, Ogino A, Ohno T, Kondo T, Nakagawa M, Minatoguchi S, Fujiwara T, Fujiwara H.** ANG II type 1A receptor signaling causes unfavorable scar dynamics in the postinfarct heart. *Am J Physiol Heart Circ Physiol* 292: H946–H953, 2007.
22. **Liu Y, Leri A, Li B, Wang X, Cheng W, Kajstura J, Anversa P.** Angiotensin II stimulation in vitro induces hypertrophy of normal and postinfarcted ventricular myocytes. *Circ Res* 82: 1145–1159, 1998.
23. **Massie BM, Carson PE, McMurray JJ, Komajda M, McKelvie R, Zile MR, Anderson S, Donovan M, Iverson E, Staiger C, Ptaszynska A.** Irbesartan in patients with heart failure and preserved ejection fraction. *N Engl J Med* 359: 2456–2467, 2008.
24. **Matsubara LS, Matsubara BB, Okoshi MP, Cicogna AC, Janicki JS.** Alterations in myocardial collagen content affect rat papillary muscle function. *Am J Physiol Heart Circ Physiol* 279: H1534–H1539, 2000.
25. **Morales C, Gonzalez GE, Rodriguez M, Bertolasi CA, Gelpi RJ.** Histopathologic time course of myocardial infarct in rabbit hearts. *Cardiovasc Pathol* 11: 339–345, 2002.
26. **Opie LH, Commerford PJ, Gersh BJ, Pfeffer MA.** Controversies in ventricular remodelling. *Lancet* 367: 356–367, 2006.
27. **Patten RD, Aronovitz MJ, Einstein M, Lambert M, Pandian NG, Mendelsohn ME, Konstam MA.** Effects of angiotensin II receptor blockade versus angiotensin-converting-enzyme inhibition on ventricular remodelling following myocardial infarction in the mouse. *Clin Sci (Lond)* 104: 109–118, 2003.
28. **Pfeffer MA, McMurray J, Leizorovicz A, Maggioni AP, Rouleau JL, Van De WF, Henis M, Neuhart E, Gallo P, Edwards S, Sellers MA, Velazquez E, Califf R.** Valsartan in Acute Myocardial Infarction Trial (VALIANT): rationale and design. *Am Heart J* 140: 727–750, 2000.
29. **Pitt B, Poole-Wilson PA, Segal R, Martinez FA, Dickstein K, Camm AJ, Konstam MA, Riegger G, Klinger GH, Neaton J, Sharma D, Thiyagarajan B.** Effect of losartan compared with captopril on mortality in patients with symptomatic heart failure: randomised trial–the Losartan Heart Failure Survival Study ELITE II. *Lancet* 355: 1582–1587, 2000.
30. **Pourdjabbar A, Parker TG, Nguyen QT, Desjardins JF, Lapointe N, Tsoporis JN, Rouleau JL.** Effects of pre-, peri-, and postmyocardial infarction treatment with losartan in rats: effect of dose on survival, ventricular arrhythmias, function, and remodeling. *Am J Physiol Heart Circ Physiol* 288: H1997–H2005, 2005.
31. **Richer C, Fornes P, Cazaubon C, Domergue V, Nisato D, Giudicelli JF.** Effects of long-term angiotensin II AT_1 receptor blockade on survival, hemodynamics and cardiac remodeling in chronic heart failure in rats. *Cardiovasc Res* 41: 100–108, 1999.
32. **Sandmann S, Li J, Fritzenkotter C, Spormann J, Tiede K, Fischer JW, Unger T.** Differential effects of olmesartan and ramipril on inflammatory response after myocardial infarction in rats. *Blood Press* 15: 116–128, 2006.
33. **Shimizu T, Okamoto H, Chiba S, Matsui Y, Sugawara T, Akino M, Nan J, Kumamoto H, Onozuka H, Mikami T, Kitabatake A.** VEGF-mediated angiogenesis is impaired by angiotensin type 1 receptor blockade in cardiomyopathic hamster hearts. *Cardiovasc Res* 58: 203–212, 2003.
34. **Simko F, Simko J, Fabryova M.** ACE-inhibition and angiotensin II receptor blockers in chronic heart failure: pathophysiological consideration of the unresolved battle. *Cardiovasc Drugs Ther* 17: 287–290, 2003.
35. **Sugano Y, Anzai T, Yoshikawa T, Maekawa Y, Kohno T, Mahara K, Naito K, Ogawa S.** Granulocyte colony-stimulating factor attenuates early ventricular expansion after experimental myocardial infarction. *Cardiovasc Res* 65: 446–456, 2005.
36. **Sun Y, Zhang JQ, Zhang J, Ramires FJ.** Angiotensin II, transforming growth factor-beta1 and repair in the infarcted heart. *J Mol Cell Cardiol* 30: 1559–1569, 1998.
37. **Tanimura M, Sharov VG, Shimoyama H, Mishima T, Levine TB, Goldstein S, Sabbah HN.** Effects of AT_1-receptor blockade on progression of left ventricular dysfunction in dogs with heart failure. *Am J Physiol Heart Circ Physiol* 276: H1385–H1392, 1999.
38. **Thai HM, Van HT, Gaballa MA, Goldman S, Raya TE.** Effects of AT_1 receptor blockade after myocardial infarct on myocardial fibrosis, stiffness, and contractility. *Am J Physiol Heart Circ Physiol* 276: H873–H880, 1999.
39. **van Kats JP, Duncker DJ, Haitsma DB, Schuijt MP, Niebuur R, Stubenitsky R, Boomsma F, Schalekamp MA, Verdouw PD, Danser AH.** Angiotensin-converting enzyme inhibition and angiotensin II type 1 receptor blockade prevent cardiac remodeling in pigs after myocardial infarction: role of tissue angiotensin II. *Circulation* 102: 1556–1563, 2000.
40. **Vanhoutte D, Schellings M, Pinto Y, Heymans S.** Relevance of matrix metalloproteinases and their inhibitors after myocardial infarction: a temporal and spatial window. *Cardiovasc Res* 69: 604–613, 2006.
41. **Xia QG, Chung O, Spitznagel H, Illner S, Janichen G, Rossius B, Gohlke P, Unger T.** Significance of timing of angiotensin AT_1 receptor blockade in rats with myocardial infarction-induced heart failure. *Cardiovasc Res* 49: 110–117, 2001.
42. **Xu X, Wan W, Ji L, Lao S, Powers AS, Zhao W, Erikson JM, Zhang JQ.** Exercise training combined with angiotensin II receptor blockade limits post-infarct ventricular remodelling in rats. *Cardiovasc Res* 78: 523–532, 2008.

43. **Yamagishi H, Kim S, Nishikimi T, Takeuchi K, Takeda T.** Contribution of cardiac renin-angiotensin system to ventricular remodelling in myocardial-infarcted rats. *J Mol Cell Cardiol* 25: 1369–1380, 1993.
44. **Yusuf S, Pfeffer MA, Swedberg K, Granger CB, Held P, McMurray JJ, Michelson EL, Olofsson B, Ostergren J.** Effects of candesartan in patients with chronic heart failure and preserved left-ventricular ejection fraction: the CHARM-Preserved Trial. *Lancet* 362: 777–781, 2003.
45. **Zdrojewski T, Gaudron P, Whittaker P, Poelzl S, Schiemann J, Hu K, Ertl G.** Ventricular remodeling after myocardial infarction and effects of ACE inhibition on hemodynamics and scar formation in SHR. *Cardiovasc Pathol* 11: 88–93, 2002.